

Novel Paracellin-1 Mutations in 25 Families with Familial Hypomagnesemia with Hypercalciuria and Nephrocalcinosis

STEFANIE WEBER,* LINDA SCHNEIDER,* MELANIE PETERS,*
 JOACHIM MISSELWITZ,† GABRIELE RÖNNEFARTH,† MICHAEL BÖSWALD,‡
 KLAUS E. BONZEL,§ TOMAS SEEMAN,|| TEREZA SULÁKOVÁ,¶
 EBERHARD KUWERTZ-BRÖKING,# ALOJZ GREGORIC,**
 JEAN-BERNARD PALCOUX,†† VELIBOR TASIC,‡‡ FRIEDRICH MANZ,§§
 KARL SCHÄRER,||| HANNSJÖRG W. SEYBERTH,* and MARTIN KONRAD*

*Department of Pediatrics, Philipps University, Marburg, Germany; †Department of Pediatrics, University Hospital, Jena, Germany; ‡Department of Pediatrics, University Hospital, Erlangen, Germany; §Department of Pediatrics, University Hospital, Essen, Germany; ||Department of Pediatrics, University Hospital, Prague, Czech Republic; ¶Department of Pediatrics, University Hospital, Ostrava, Czech Republic; #Department of Pediatrics, University Hospital, Münster, Germany; **Department of Pediatrics, University Hospital, Maribor, Slovenia; ††Department of Pediatrics, University Hospital, Clermont-Ferrand, France; ‡‡Clinic for Children's Diseases, Skopje, Macedonia; §§Research Institute of Child Nutrition, Dortmund, Germany; and |||Department of Pediatrics, University Hospital, Heidelberg, Germany.

Abstract. Familial hypomagnesemia with hypercalciuria and nephrocalcinosis (FHHNC) is an autosomal recessive tubular disorder that is frequently associated with progressive renal failure. The primary defect is related to impaired tubular reabsorption of magnesium and calcium in the thick ascending limb of Henle's loop. Mutations in *PCLN-1*, which encodes the renal tight junction protein paracellin-1 (claudin-16), were identified as the underlying genetic defects. Comprehensive clinical data and the results of *PCLN-1* mutation analysis of 25 FHHNC families with 33 affected individuals are presented. Patients presented mainly with urinary tract infections, polyuria, and hematuria at a median age of 3.5 yr. At the time of diagnosis, the GFR was already decreased to <60 ml/min per 1.73 m² for 11 patients. Twelve patients exhibited progression

to end-stage renal disease, at a median age of 14.5 yr. Treatment with magnesium salts and thiazides seemed to have no effect on the progression of the disease. Genotype analysis revealed *PCLN-1* mutations in all except three mutant alleles (94%). Fifteen different mutations were observed, including eight novel mutations. The accumulation of mutations affecting the first extracellular loop was striking, with 48% of all mutant alleles exhibiting a Leu151Phe exchange. Haplotype analysis strongly suggested a founder effect among patients with FHHNC who originated from Germany or eastern European countries. In 13 of 23 families, hypercalciuria and/or nephrolithiasis were observed in otherwise unaffected family members, indicating a possible role of heterozygous *PCLN-1* mutations in yielding hypercalciuric stone-forming conditions.

Hereditary renal diseases associated with magnesium loss comprise a set of rare tubular disorders with different modes of inheritance (reviewed in reference 1), including isolated renal magnesium loss [Mendelian Inheritance in Man (MIM) 154020 and MIM 248250] (2), Gitelman syndrome (MIM 263800) (3), and autosomal recessive familial hypomagnesemia with hypercalciuria and nephrocalcinosis (FHHNC) (MIM 248250 and MIM 603959). FHHNC was first described by Michelis *et al.* (4) in 1972 (Michelis-Castrillo syndrome) (5). Since then, patients of at

least 50 different FHHNC kindreds have been reported (reviewed in references 6–9).

In contrast to primary hypomagnesemia and Gitelman syndrome, FHHNC is generally complicated by chronic renal failure (CRF) in early childhood or adolescence. Recurrent urinary tract infections (UTI) and polyuria/polydipsia are frequent initial symptoms. In addition to marked hypomagnesemia, all affected individuals exhibit hypercalciuria and nephrocalcinosis. Additional symptoms at manifestation include nephrolithiasis, abdominal pain, convulsions, muscular tetany, failure to thrive, incomplete distal renal tubular acidosis (dRTA), and hypocitraturia (10–12). Some authors reported elevated serum parathyroid hormone (PTH) levels early in the course of the disease, independently of GFR (12). Hyperuricemia was observed for the majority of patients (12–14). Ocular abnormalities and hearing impairment have been reported as inconsistent extrarenal findings (6). In one report, histories of hypercalciuria and kidney stones were frequently noted for otherwise healthy family members (12).

Received December 18, 2000. Accepted February 23, 2001.

Correspondence to Dr. Martin Konrad, Department of Pediatrics, Philipps University, Deutschhausstrasse 12, D-35037 Marburg, Germany. Phone: 49-6421-2862789; Fax: 49-6421-2868956; E-mail: konradm@mail.uni-marburg.de

1046-6673/1209-1872

Journal of the American Society of Nephrology

Copyright © 2001 by the American Society of Nephrology

Clinical observations and clearance studies performed with patients with FHHNC point to impaired reabsorption of magnesium and calcium in the thick ascending limb of Henle's loop (TAL) as the primary tubular defect (14). The TAL plays a predominant role in the renal reabsorption of divalent cations, which mainly pass via paracellular flux in this nephron segment (15). Mutations in the *PCLN-1* gene were recently identified as the underlying genetic defects in FHHNC (7). *PCLN-1* encodes paracellin-1 (claudin-16), a newly identified, tight junction protein of the claudin multigene family that is expressed in the TAL and the distal convoluted tubule. The claudin family comprises a set of structurally related proteins involved in the formation of tight junction strands in various tissues (16). In addition to claudins, multiple proteins of different classes have been identified in tight junctions, and protein assembly seems to be complex. The definite structure of paracellin-1 is not yet well defined, because there are uncertainties regarding the amino-terminal length of the protein. Mutation analysis among disease-affected individuals is a possible way to gain further insight into this issue. Here we present comprehensive genotypic data on 25 FHHNC families with 33 affected individuals, and we provide detailed information regarding phenotypic presentations and clinical courses for this large, genetically characterized cohort.

Materials and Methods

Patients and Families

Twenty-five FHHNC families of different ethnic origins, with 33 affected individuals who were treated in 12 European pediatric departments, were analyzed in this study (Table 1). Family pedigrees are shown in Figure 1. Clinical aspects of families F1 (10) and F10 (9) were reported previously, and genotypic data for families F1 to F8 were presented earlier by our group (8). For all patients, diagnosis was based on the following required symptoms: hypomagnesemia, hypercalciuria, bilateral nephrocalcinosis, and the absence of hypokalemic metabolic alkalosis.

Parental consanguinity was noted for four families. Eight families were multiplex, with two affected siblings. In one of these families (F14), there were uniovular twins. This study was approved by the local ethics committee, and informed consent was obtained from the patients and/or their parents.

Clinical and Laboratory Data

Serum levels of magnesium, calcium, potassium, creatinine, PTH, and uric acid and acid-base status were analyzed using standard techniques. Additional parameters evaluated included urinary excretion of magnesium, calcium, and citrate and urinary acidification capability. Hypomagnesemia was defined as repeated serum magnesium levels of <0.65 mM (17). Calcium excretion was expressed either as milligrams per kilogram per 24 h or as the urinary calcium/creatinine ratio. Urinary calcium excretion of >4 mg/kg per 24 h was considered hypercalciuric for children >2 yr of age (18). The age-dependent upper reference values for urinary calcium/creatinine ratios for young children were based on the evaluations by Matos *et al.* (19). The GFR was calculated for 30 patients from serum creatinine levels and body heights, using the formula described by Schwartz *et al.* (20). CRF was defined as GFR of <60 ml/min per 1.73 m².

The onset and presence of polyuria/polydipsia, UTI, nephrolithiasis, and other symptoms of FHHNC were documented. In addition, the

results of renal sonography, radiography, and/or computer tomography were recorded.

Family histories were analyzed for 23 families, focusing on hypercalciuria, nephrocalcinosis, nephrolithiasis, and recurrent UTI. For first-degree family members and FHHNC-unaffected siblings, urinary calcium excretion was examined and renal ultrasonography was performed. For adult individuals, hypercalciuria was defined as a urinary calcium/creatinine ratio of >0.6 mmol/mmol.

Mutation Analysis

PCLN-1 mutation screening was performed by single-strand conformation polymorphism analysis (21). An overlapping set of primers (7) based on the sequence of the human *PCLN-1* gene was used to amplify the coding sequence (exons 1 to 5) of genomic DNA by PCR. Amplified products were separated on polyacrylamide gels by electrophoresis (Multiphor II; Pharmacia Biotech, Uppsala, Sweden). Subsequently, exons with conformational variants were directly sequenced using corresponding sequencing primers (ALFexpress DNA sequencer; Pharmacia Biotech).

Haplotype Analysis

The microsatellite markers D3S1294, D3S1314, D3S1288, D3S2747 (22), and 539-5 (7), linked to the *PCLN-1* gene on chromosome 3q27, were amplified by PCR using primer pairs as reported (with Cy5-labeled forward primers). Fragments were separated on 6% polyacrylamide gels run under denaturing conditions in an ALFexpress DNA sequencer (Pharmacia Biotech), and data were analyzed using Fragment Manager software version 1.2 (Pharmacia Biotech). Alleles were numbered according to their order in gel electrophoresis, and haplotypes were constructed from the genotypic data. The most likely haplotypes were inferred by minimizing the number of crossover events in each family.

Statistical Analyses

Statistical analyses of the paracellin-1 structure and amino acid composition, sequence alignments, and similarity searches were conducted using software provided by Infobiogen (www.infobiogen.fr) and the National Center for Biotechnical Information (www.ncbi.nlm.nih.gov).

Results

Clinical Presentation

Table 1 summarizes the clinical and genotypic data. There were 20 female patients and 13 male patients in the cohort. Ages at the time of the initial manifestation ranged from 2 mo to 18 yr, with a median age of 3.5 yr ($n = 30$). Recurrent UTI, polyuria/polydipsia, hematuria, and abacterial leukocyturia were the most frequent presenting symptoms (Table 2). Few patients presented with nephrolithiasis, cerebral convulsions, muscular tetany, or abdominal pain. In multiplex families, diagnosis of the disease for one sibling generally prompted the search for FHHNC in the other sibling. For one patient (patient F21-1), nephrocalcinosis was detected incidentally by abdominal sonography during evaluation of a gastrointestinal infection at the age of 3 mo; further clinical evaluation revealed hypomagnesemia, hypercalciuria, and polyuria.

Ten patients were affected by different eye lesions (Table 1). Hearing impairment was not noted for any of the patients in this study cohort. Differential diagnoses included idiopathic

Table 1. Characteristics of the patient cohort^a

Patient No.	Gender	Origin	Consanguinity	Zygoty	Nucleotide Change	Consequence of Mutation	Age at Manifestation	Age at Time of Study	Current Renal Function	Lowest Serum Mg ²⁺ Concentration (mM)	Nephrolithiasis	UTI	Eye Lesions
F1-1	F	German	–	Comp hetero	350(TGG→TAG)-453(TTG→TTT)	Trp117X-Leu151Phe	2 mo	41 yr	Tx	0.40	ND	+	–
F1-2	F	German	–	Comp hetero	350(TGG→TAG)-453(TTG→TTT)	Trp117X-Leu151Phe	7 yr	39 yr	Tx	0.46	+	+	–
F2-1	F	German	–	Comp hetero	453(TTG→TTT)-453(TTG→TGG)	Leu151Phe-Leu151Trp	18 yr	42 yr	Tx	0.23	+	+	–
F2-2	M	German	–	Comp hetero	453(TTG→TTT)-453(TTG→TGG)	Leu151Phe-Leu151Trp	12 yr	36 yr	Tx	0.40	–	–	–
F3	F	Turkish	+	Homo	593(GGT→GCT)	Gly198Ala	6 mo	24 yr	CRF	0.40	–	+	S
F4	F	Tunesian	+	Homo-(homo)	715(GGA→AGA)-166del(GG)→ins(C)	Gly239Arg-Arg55fs	4 yr	21 yr	Dialysis	0.25	–	–	M, A
F5-1	F	German	–	Comp hetero	434(CTG→CCG)-453(TTG→TTT)	Leu145Pro-Leu151Phe	4 yr	17 yr	GFR>60	0.48	–	–	–
F5-2	F	German	–	Comp hetero	434(CTG→CCG)-453(TTG→TTT)	Leu145Pro-Leu151Phe	7 yr	20 yr	GFR>60	0.50	–	–	–
F6	M	Bosnian	–	Comp hetero	453(TTG→TTT)-715(GGA→AGA)	Leu151Phe-Gly239Arg	6 yr	14 yr	GFR>60	0.30	ND	–	–
F7-1	M	Czech	–	Homo	453(TTG→TTT)	Leu151Phe	4 yr	11 yr	CRF	0.51	+	+	H, A
F7-2	M	Czech	–	Homo	453(TTG→TTT)	Leu151Phe	9 mo	8 yr	CRF	0.43	+	+	–
F8-1	M	Tunesian	+	Homo-(homo)	421(CAT→GAT)-165/166del(GG)→ins(C)	His141Asp-Arg55fs	18 mo	5 yr	Dialysis	0.55	–	+	–
F8-2	F	Tunesian	+	Homo-(homo)	421(CAT→GAT)-165/166del(GG)→ins(C)	His141Asp-Arg55fs	4 yr	8 yr	CRF	0.46	–	+	–
F9-1	F	Algerian	+	Homo	646/647(CGT→ACT)	Arg216Thr	ND	23 yr	CRF	0.49	–	+	–
F9-2	M	Algerian	+	Homo	646/647(CGT→ACT)	Arg216Thr	ND	28 yr	Tx	ND ^b	–	+	ND
F10	F	Slovenian	–	Homo	434(CTG→CCG)	Leu145Pro	7 yr	16 yr	CRF	0.28	+	+	M
F11	F	Adopted child	ND	Homo	715(GGA→AGA)	Gly239Arg	ND	13 yr	CRF	0.48	–	+	–
F12	M	German	–	Comp hetero	453(TTG→TTT)-625(GCT→ACT)-165/166del(GG)→ins(C)	Leu151Phe-Ala209Thr-Arg55fs	11 yr	14 yr	GFR>60	0.40	–	–	–
F13	M	German	–	Homo	453(TTG→TTT)	Leu151Phe	2 mo	9 yr	CRF	0.43	–	–	–
F14-1	F	German	–	Homo	453(TTG→TTT)	Leu151Phe	3 yr	15 yr	Tx	0.23	–	–	–
F14-2	F	German	–	Homo	453(TTG→TTT)	Leu151Phe	3 yr	15 yr	CRF	0.30	+	+	M
F15	F	German	–	Homo	446(CGA→CTA)	Arg149Leu	6 yr	25 yr	Tx	0.42	ND	+	–
F16	F	German	–	Comp hetero	453(TTG→TTT)-785-14(T→G)	Leu151Phe-Splice site mutation	3 yr	28 yr	Dialysis	0.31	+	+	M
F17	F	German	–	Homo	453(TTG→TTT)	Leu151Phe	1 yr	17 yr	CRF	0.38	–	+	–
F18	F	German	–	Homo	453(TTG→TTT)	Leu151Phe	9 yr	17 yr	GFR>60	0.33	–	–	–
F19	M	German	–	Hetero	325-5(T→G)	Splice site mutation	5 yr	23 yr	Dialysis	0.57	+	+	–
F20	M	Polish	–	Comp hetero	434(CTG→CCG)-453(TTG→TTT)	Leu145Pro-Leu151Phe	2 yr	14 yr	Tx	0.61	–	–	M
F21-1	M	Czech	–	Comp hetero	368del(A)-434(CTG→CCG)	Asn123fs-Leu145Pro	3 mo	6 yr	GFR>60	0.40	–	+	–
F21-2	F	Czech	–	Comp hetero	368del(A)-434(CTG→CCG)	Asn123fs-Leu145Pro	2 mo	3 yr	GFR>60	0.58	–	+	–
F22	M	German	–	Homo	453(TTG→TTT)	Leu151Phe	9 mo	10 yr	GFR>60	0.46	+	+	M
F23	M	Czech	–	Comp hetero	453(TTG→TTT)-703(TCC→CCC)	Leu151Phe-Ser235Pro	6 mo	13 yr	CRF	0.40	–	+	–
F24	F	French	–	–	No mutation in coding sequence	No mutation in coding sequence	3 yr	15 yr	GFR>60	0.27	–	–	ND
F25	M	Macedonian	–	Homo	453(TTG→TTT)	Leu151Phe	7 mo	10 mo	GFR>60	0.40	–	+	–

F, female; M, male; Comp hetero, compound heterozygous; Homo, homozygous; del, deletion; ins, insertion; X, stop codon; fs, frameshift; GFR>60, GFR of >60 ml/min per 1.73 m² [calculated as described (20)]; CRF, chronic renal failure (GFR of <60 ml/min per 1.73 m²); Tx, renal transplantation; UTI, urinary tract infection; ND, no data; S, strabism; M, myopia; A, astigmatism; H, hypermetropia.

^aDNA nucleotide and amino acid position numbering was according to EMBL/GenBank/DDBJ accession no. AF152101.

^bNo pretransplant serum-Mg²⁺ concentration data were available; the diagnosis was based on clinical findings and data for sibling F9-1.

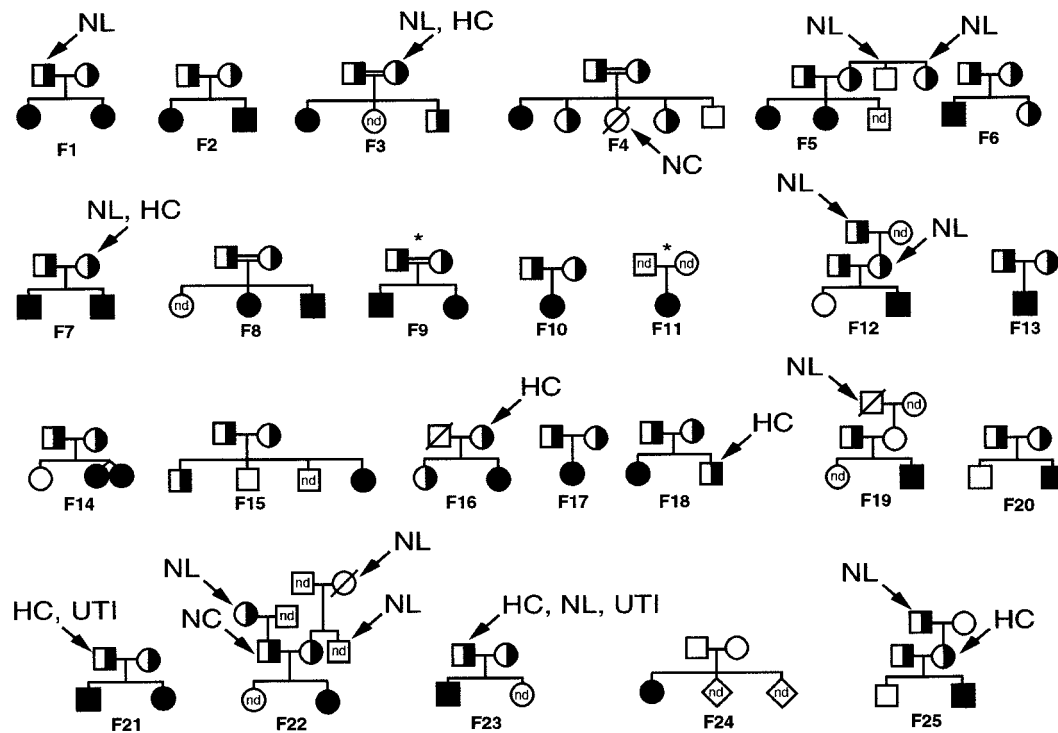


Figure 1. Family pedigrees for families F1 to F25 and results of family studies. Family members affected by hypercalciuria (HC), nephrolithiasis (NL), nephrocalcinosis (NC), and/or recurrent urinary tract infections (UTI) are indicated by arrows. Filled symbols, affected individuals; half-filled symbols, heterozygous mutation carriers. Individuals for whom blood samples were not available are labeled nd (no data). Two families were not examined (indicated by *).

hypercalciuria, medullary sponge kidneys, Dent's disease, and hyperprostaglandin E syndrome/antenatal Bartter syndrome.

Biochemical Data and Renal Function

The minimal serum magnesium value for each patient is presented in Table 1. The lowest serum magnesium level noted was <0.65 mM for all patients. The median value of the lowest serum magnesium levels was 0.40 mM ($n = 32$). Serum calcium levels were <1.8 mM at any time for 8 patients, 1.8 to 2.2 mM for 8 patients, and >2.2 mM for 14 patients. Two hypocalcemic patients exhibited signs of rickets in the neonatal period. The median maximal urinary calcium excretion value was 10.0 mg/kg per 24 h ($n = 27$). When measured for the first time, GFR was >80 ml/min per 1.73 m² for 7 patients, 60 to 80 ml/min per 1.73 m² for 13 patients, and <60 ml/min per 1.73 m² for 11 affected children (Figure 2).

Renal Sonographic and Histologic Results

For all patients, advanced bilateral nephrocalcinosis with characteristic medullary distribution was observed early in the course of the disease, independently of GFR. Renal cysts were observed for five patients. Renal histologic findings, which were documented for 11 patients, demonstrated calcium deposits, glomerular sclerosis, immature glomeruli, tubular atrophy, and interstitial fibrosis to a variable extent.

Clinical Course

Clinical symptoms and laboratory data recorded during the follow-up period are summarized in Table 3. The median of follow-up was 7 yr, with a range of 0.5 to 25.5 yr. The majority of patients developed polyuria, polydipsia, and UTI. For most patients examined, we observed elevated serum PTH levels, incomplete dRTA, hypocitraturia, and hyperuricemia.

Figure 2 demonstrates that progression to CRF was variable. Patient F8-1 exhibited the most rapid decline in renal function, beginning with a GFR of 33 ml/min per 1.73 m² at the age of 3 yr and reaching end-stage renal disease (ESRD) at 5.5 yr of age. In contrast, patients F1-2 and F2-1 attained ESRD late, at 34 and 37.5 yr of age, respectively. Several other patients also exhibited protracted courses.

By the end of the follow-up period, 12 patients (36%) had reached ESRD. The median age at the time of ESRD was 14.5 yr (range, 5.5 to 37.5 yr; one patient's age missing). Four patients were receiving dialysis treatment, and eight patients had undergone transplantation. Eleven patients (33%) exhibited GFR of <60 ml/min per 1.73 m², whereas ten patients (31%) still exhibited GFR of >60 ml/min per 1.73 m². Treatment with magnesium salts (to supplement renal loss) and thiazides (to reduce urinary calcium excretion rates) for the majority of patients apparently failed to prevent the progression of the disease.

Mutation Analysis of PCLN-1

Mutation analysis of *PCLN-1* by single-strand conformation polymorphism analysis and direct sequencing revealed 15 different mutations among our cohort of 25 families (Table 1). Both mutant *PCLN-1* alleles were detected in all affected individuals, with two exceptions; only a heterozygous splice site mutation was observed for patient F19, although the complete coding region and the adjacent intronic sequences were analyzed, and no *PCLN-1* mutation was detected for patient

F24. Figure 3 depicts affected amino acid residues in the paracellin-1 protein.

In addition to the mutations described previously, eight novel *PCLN-1* mutations were identified, including five missense mutations, one frameshift mutation, and two splice site mutations. All mutations cosegregated with the phenotype, and none of the single-nucleotide exchanges was observed in at least 100 control chromosomes.

Of the mutant alleles, 31 of 46 (67%) exhibited a missense

Table 2. Initial clinical presentation

Symptoms at Manifestation	No. of Patients
Urinary tract infection	13/30 (43%)
Polyuria/polydipsia	8/30 (27%)
Hematuria	6/30 (20%)
Abacterial leukocyturia	5/30 (17%)
Nephrolithiasis	4/30 (13%)
Failure to thrive	4/30 (13%)
Cerebral convulsions	4/30 (13%)
Abdominal pain	3/30 (10%)
Vomiting/feeding problems	3/30 (10%)
Rickets	2/30 (7%)
Muscular tetany	2/30 (7%)
Enuresis	1/30 (3%)
Incidental detection	1/30 (3%)
Examination because of affected sibling	4/30 (13%)

Table 3. Clinical and biochemical findings observed during the follow-up period^a

Symptoms	No. of Patients
Hypomagnesemia	33/33 (100%)
Hypercalciuria	33/33 (100%)
Nephrocalcinosis	33/33 (100%)
Polyuria/polydipsia	28/31 (90%)
Increased serum iPTH levels	22/25 (88%)
Incomplete dRTA	17/20 (85%)
Hypocitraturia	12/15 (80%)
Urinary tract infection	22/32 (69%)
Hyperuricemia	18/28 (64%)
Muscular tetany	10/30 (33%)
Nephrolithiasis	10/31 (32%)
Ocular pathologic conditions	8/31 (26%)
Cerebral convulsions	5/30 (17%)
Hearing impairment	0/33 (0%)

^a iPTH, intact parathyroid hormone; dRTA, distal renal tubular acidosis.

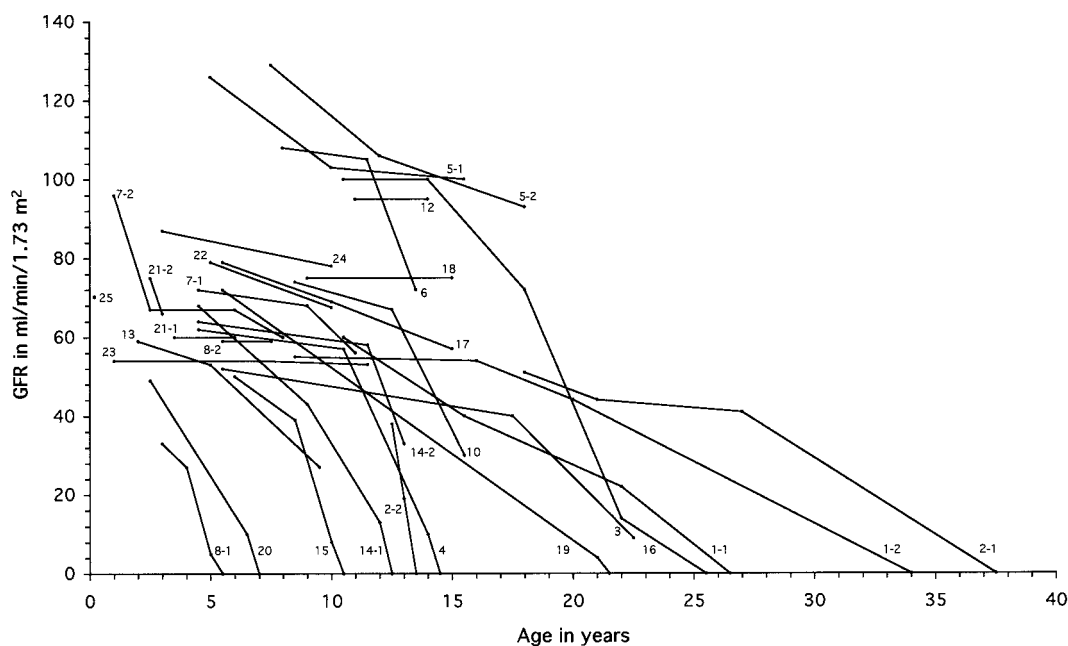


Figure 2. Changes in GFR for 30 patients affected by familial hypomagnesemia with hypercalciuria and nephrocalcinosis (FHHNC). The GFR of FHHNC-affected patients during their clinical courses are presented. The GFR was calculated as described (20). At the onset of end-stage renal disease, dialysis was initiated or renal transplantation was performed.

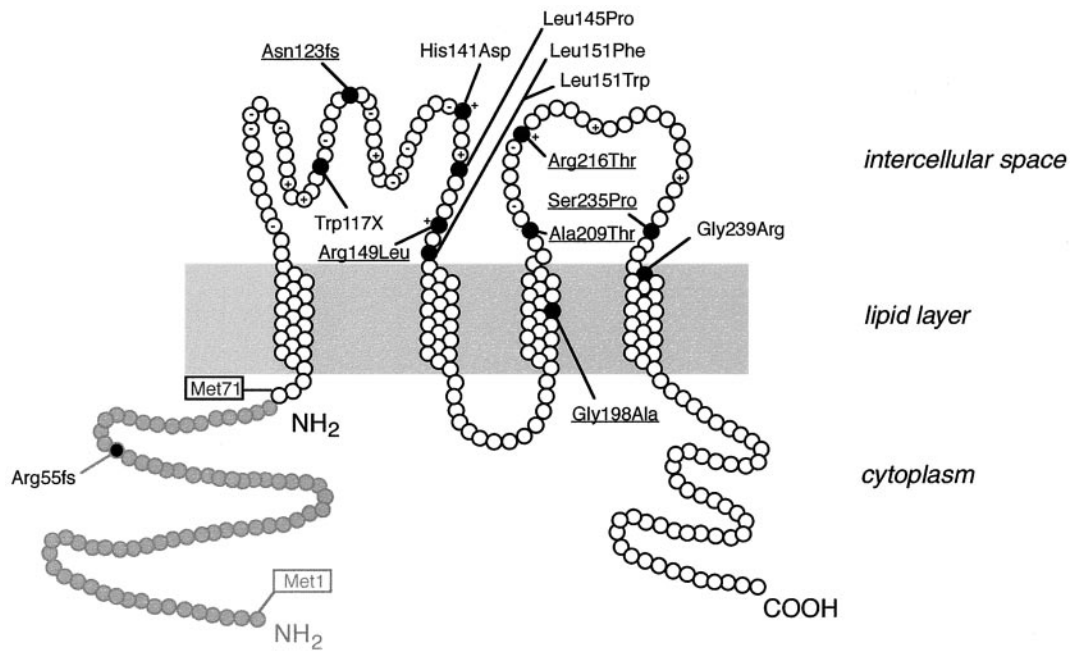


Figure 3. Paracellin-1 protein model deduced from hydrophilicity plots. Amino acid residues affected by *PCLN-1* mutations in the cohort of families F1 to F25 are depicted in black (novel *PCLN-1* mutations are underlined). Two newly identified splice site mutations are not shown. Charged wild-type amino acids in the extracellular loops are marked. On the basis of the results of mutation analysis and sequence comparisons, the paracellin-1 protein seems to be shorter than reported previously (the 70 amino-terminal amino acids that are presumably lacking are depicted in gray). Both translational start sites are shown.

mutation affecting the first extracellular loop of paracellin-1. Amino acid sequence alignments with other members of the claudin multigene family revealed the highest degree of homology in this part of the protein, and Leu145Pro, Arg149Leu, Leu151Thr, and Leu151Phe mutations all affected highly conserved amino acid residues in this loop. In total, 22 of 46 mutant alleles (48%) were affected by a Leu151Phe exchange. Haplotype analysis with microsatellite markers flanking the *PCLN-1* gene [D3S1294, D3S1314, D3S1288, D3S2747 (22), and 539-5 (7)] and analysis of an intronic polymorphism in the *PCLN-1* gene (intron 1/2, splice 325+61T→C) were subsequently performed. Results revealed a common extended haplotype that was shared by 50% (nine of 18) of the Leu151Phe-affected alleles but was not present in 72 unaffected control alleles (Figure 4). The highly polymorphic marker D3S1314 was mapped to the genomic clone of EMBL/GenBank/DDBJ accession no. AC009520, which also comprises the 5' end of the human *PCLN-1* gene, defining a physical distance between D3S1314 and *PCLN-1* of 13.7 kb. All Leu151Phe-affected chromosomes exhibited the same allele (numbered as allele 6) for marker D3S1314. In contrast, only 17% of control chromosomes exhibited this allele. This finding strongly suggests a founder effect for the Leu151Phe mutation.

In three families (F4, F8, and F12), a frameshift mutation affecting amino acid residue Arg55 was identified, in addition to a missense mutation further 3' downstream on the same chromosome. The Arg55fs mutation was caused by deletion of two guanine residues (G165/G166) and insertion of a single cytosine residue (C165). This mutation affects the amino-

terminal part of the protein, leading to premature termination at position 90. Unexpectedly, analysis of 72 control chromosomes revealed a frequency of the G165/G166 deletion-C165 insertion of 16.7% (12 of 72 chromosomes), indicating a common polymorphism rather than a pathogenic mutation.

Genotype-Phenotype Relationship and Intrafamilial Variability

Phenotypic evaluation with respect to the results of the mutation analysis revealed no obvious genotype-phenotype relationship. However, with respect to the progression of renal failure, we observed a rather close intrafamilial phenotypic concordance, with a mild clinical course for the siblings of family F5, an intermediate course for patients of families F1, F9, and F21, and a more severe course for patients of families F7 and F14 (uniovular twins) (Figure 2). In contrast, the siblings of family F2 differed in disease severity, reaching ESRD at the ages of 13.5 and 37 yr. Similarly, the younger sibling of patient F8 began dialysis treatment at 5.5 yr of age, whereas his sister, who was 8 yr of age at the end of the follow-up period, maintained a stable GFR of 60 ml/min per 1.73 m².

Family Histories

Histories of nephrolithiasis, nephrocalcinosis, and/or hypercalciuria were observed for 13 of 23 families (56%), with nephrolithiasis being the most frequent finding. Detailed results are presented in Figure 1.

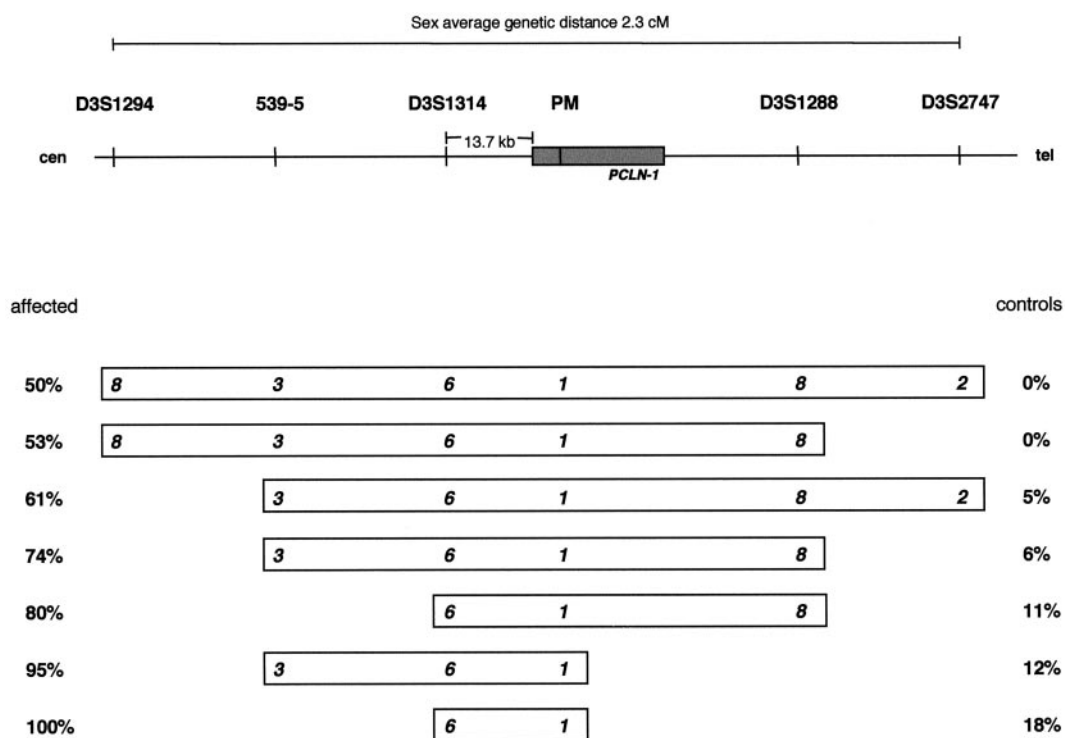


Figure 4. Founder effect of Leu151Phe, demonstrated by extended haplotype analysis. The prevalence of an extended haplotype in Leu151Phe-affected chromosomes, compared with unaffected control chromosomes, is presented. Alleles are numbered according to their order after gel electrophoresis. The numbers of different alleles for each marker were as follows: D3S1294, $n = 11$; 539-5, $n = 9$; D3S1314, $n = 12$; D3S1288, $n = 10$; D3S2747, $n = 8$. The intronic polymorphism (PM) of the *PCLN-1* gene (intron 1/2; splice 325+61T→C) was numbered 2, compared with number 1 for wild-type alleles. cen, centromere; tel, telomere.

Discussion

Phenotype Analysis

In cooperation with other European pediatric departments, we assembled a study cohort consisting of 25 FHHNC families, with 33 affected individuals, for the study of genotypes and phenotypes in FHHNC. Phenotypic evaluation of affected individuals revealed disease onset in early childhood, with recurrent UTI, polyuria/polydipsia, hematuria, and abacterial leukocyturia being the most frequently observed symptoms. In general, the final diagnosis of FHHNC was made by recognition of the triad of severe hypomagnesemia, marked hypercalciuria, and nephrocalcinosis. According to our data, 33% of the patients presented with reduced GFR (<60 ml/min per 1.73 m²) at the time of diagnosis. At the end of the follow-up period, 36% of the patients exhibited ESRD and 33% exhibited GFR of <60 ml/min per 1.73 m².

Although much progress in understanding FHHNC has been made with the identification of the genetic defect, there is still uncertainty regarding the pathophysiologic basis of renal failure in this disorder. It seems that loss or impairment of paracellin-1 function results in decreased reabsorption of magnesium in the TAL, leading to profound hypermagnesiuria and hypomagnesemia (7). Calcium and magnesium transport systems are frequently linked, as demonstrated by the paracellular pathway for both divalent cations in the TAL (15). Consequently, the defect in renal magnesium handling in FHHNC is

associated with high rates of calcium excretion. Hypercalciuria seems to play an important role in FHHNC pathophysiologic processes, contributing to the development of nephrocalcinosis and renal stone formation. In early descriptions of the disease, the degree of CRF was related to the progression of the tubulointerstitial nephropathy associated with nephrocalcinosis (14). However, different tubulopathies are accompanied by medullary nephrocalcinosis, and not all of them are followed by CRF (23). For example, in dRTA and hyperprostaglandin E syndrome/antenatal Bartter syndrome, the GFR is generally not impaired, despite severe nephrocalcinosis (23,24). Additional, currently unidentified factors seem to be important for the development of CRF in FHHNC.

With the interfamilial variability but frequent intrafamilial concordance observed for our study cohort, additional factors influencing the rate of progression of renal insufficiency might be related to the genetic backgrounds of the affected patients. Further factors include aspects of medical surveillance and patient compliance with supportive treatment.

In general, therapeutic success is poor in FHHNC. Despite continuous administration of magnesium supplements to most patients, serum magnesium levels usually remain low, with urinary magnesium excretion increasing proportionally because of the disease-specific alterations in the renal magnesium threshold and transport maximum (14). To reduce the progression of nephrocalcinosis via the correction of hypercalciuria,

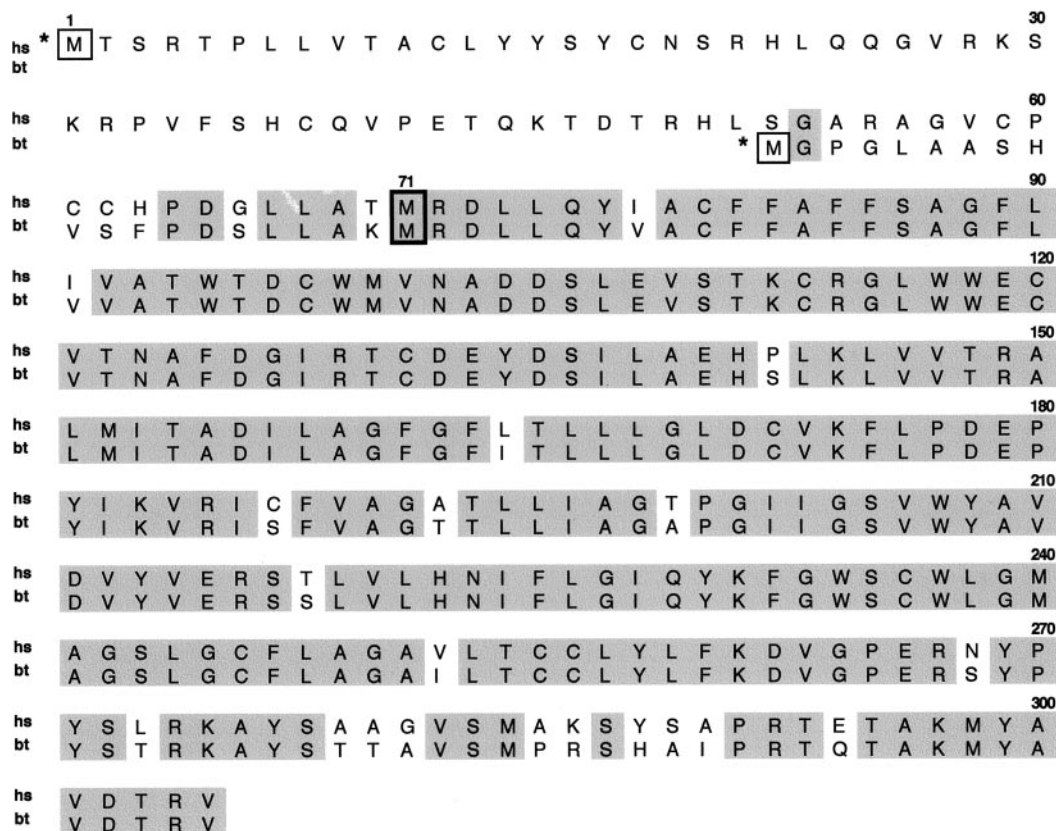


Figure 5. Amino acid sequence alignment of human paracellin-1 (EMBL/GenBank/DDBJ accession no. AF152101) and bovine paracellin-1 (EMBL/GenBank/DDBJ accession no. AB030082). Identical amino acids are shadowed in gray. Human and bovine translational start methionines, as reported in the GenBank submissions, are indicated by asterisks and thin black boxes. The proteins share a methionine in a suitable Kozak consensus sequence (human Met71/bovine Met20, marked by a thick black box), followed by a sequence of high homology (identity, 91%; similarity, 95%). hs, *Homo sapiens*; bt, *Bos taurus*. The one-letter amino acid code is used.

thiazides were administered to the majority of patients. However, no sustained reduction of hypercalciuria was achieved with this treatment. On the basis of experience with nephrogenic diabetes insipidus and Bartter-like syndromes, new therapeutic approaches for FHHNC might include the administration of indomethacin, as suggested by Monnens *et al.* (25). Supportive therapy is essential for the protection of kidney function and should include provision of sufficient fluids and effective treatment of stone formation and bacterial colonization. Because the primary defect in FHHNC seems to be restricted to the kidney, definite cures can be achieved with renal transplantation.

Evaluation of family histories, determination of urinary calcium excretion rates, and renal sonography revealed striking incidences of hypercalciuria, nephrolithiasis, and UTI among family members not affected by FHHNC (in 13 of 23 families). A comparable observation was reported by Praga *et al.* (12) in a study of five families. In nine families in the study presented here, the mother or father (both of whom were obligate carriers of heterozygous *PCLN-1* mutations) was affected by nephrolithiasis, nephrocalcinosis, and/or hypercalciuria. It seems reasonable to propose a relationship between isolated hypercalciuria and mutations in the *PCLN-1* gene. With the exception of the uncle of patient F5, further results of mutation analysis

support this hypothesis; heterozygous *PCLN-1* mutations were also observed for the hypercalciuric brother of patient F18 and the grandparents of patients F12, F22, and F25, who were affected by nephrolithiasis. It might be expected that mutation analysis of kindreds affected by familial hypercalciuria with nephrocalcinosis and/or nephrolithiasis (with an apparently dominant mode of inheritance) would demonstrate heterozygous mutations in the *PCLN-1* gene in a number of families.

Genotype Analysis

Genotyping revealed *PCLN-1* mutations in all mutant alleles of our study cohort, except for three alleles. Fifteen different mutations were found in *PCLN-1*, including eight novel mutations. Therefore, 24 different *PCLN-1* mutations have been identified to date (7,8). In this study, the first extracellular loop of the paracellin-1 protein was the region most often affected by single-nucleotide exchanges. This finding attracted attention in the first genotypic study of families F1 to F8 (8) and is now confirmed by the supplementary data of the mutation analysis for families F9 to F25. Overall, 67% of the mutant alleles demonstrated a missense mutation in the sequence encoding this loop (Table 1 and Figure 3). Because amino acid sequence alignments of paracellin-1 with other members of the claudin multigene family revealed a high degree of homology in this region of the protein, a special impor-

tance for paracellin-1 function must be proposed. Because of the large number of neutral amino acids, the first extracellular loop is predicted to bridge the intercellular space (26). Furthermore, the negative net charge of the loop of -4 (Figure 3), which is unique to paracellin-1 (in contrast to other claudins), is proposed to contribute to the cation sensitivity of the paracellular pathway in the TAL (7). The His141Asp and Arg149Leu mutations both result in a loss of positive charge. The Leu145Pro, Leu151Thr, and Leu151Phe mutations do not alter the net charge, but all affect highly conserved amino acid residues in the first extracellular loop. Essential features of the tertiary protein structure seem to be affected by these amino acid exchanges, resulting in alterations in protein function and paracellular conductance.

Of the mutant alleles, 48% were affected by a Leu151Phe substitution. The predominance of Leu151Phe-affected families originating from Germany or eastern Europe (Czech Republic, Slovenia, Bosnia, Macedonia, or Poland) is striking; 14 of 18 such families bore this mutation on at least one allele, whereas it was not observed among the families that originated from France, Algeria, Tunisia, or Turkey. Moreover, the Leu151Phe mutation was not observed in the study by Simon *et al.* (7) of ten families that originated from Spain, England, Italy, Egypt, Saudi Arabia, and Sri Lanka. These observations raised the question of whether the Leu151Phe exchange in this study is attributable to a common ancestor, in the sense of a founder effect, rather than a mutational hot spot. Subsequently performed analysis of an intragenic polymorphism and haplotype analysis of five flanking microsatellite markers strongly indicate a founder effect, because these analyses demonstrated a difference between Leu151Phe-affected and unaffected chromosomes (Figure 4). Allele 6 of the microsatellite marker D3S1314, which is 13.7 kb distant from *PCLN-1* and is highly polymorphic (with 12 different alleles), cosegregated with the Leu151Phe mutation in 100% of the cases, whereas only 17% of the control chromosomes bore this allele. The extended haplotype covering the *PCLN-1* region for a genetic distance of 2.3 cM was shared by 50% of the Leu151Phe-affected chromosomes but was not observed in any of the unaffected chromosomes. Recombination events in previous generations that are not detectable in our study cohort could explain the lack of complete concordance of the extended haplotype. Because all Leu151Phe-affected patients originated from Germany or eastern Europe and the Leu151Phe exchange was not observed in patients who originated from other countries, a founder effect seems very likely. Only four of the 19 families originating from Germany or eastern Europe were not affected by a Leu151Phe exchange. This observation will simplify genetic analysis among individuals with suspected FHHNC who originate from these countries.

With respect to the protein structure of paracellin-1, the following aspect of *PCLN-1* mutation analysis seems to be important: in three families, one mutant allele exhibited a frameshift mutation affecting amino acid residue Arg55, in addition to a missense mutation further 3' downstream. Although two mutations per affected allele have also been described for other hereditary diseases (27), it is not a common finding. This Arg55fs mutation, which is caused by deletion of

two guanine residues (G165/G166) and insertion of a single cytosine residue (C165), affects the amino-terminal part of the protein, producing a premature stop codon at position 90. Therefore, all missense mutations further 3' downstream do not seem to be responsible for causing disease. Kozak (28) described specific nucleotide sequences surrounding the methionine-encoding ATG start codon that promote the initiation of translation. Interestingly, as Simon *et al.* (7) have discussed, the *PCLN-1* gene encodes a second methionine (Met71) in the context of a more suitable Kozak consensus sequence, compared with Met1 (70 amino acids 3' downstream), that is in a position analogous to the start site of other claudins (16,26). It is not currently known whether this second methionine is the original translational start site. To investigate this issue, we analyzed the G165/G166 deletion-C165 insertion in 72 control chromosomes and observed its appearance with a frequency of 16.7% (12 of 72 chromosomes). Moreover, it was observed in a homozygous state in one control individual. This high prevalence in a healthy population supports the assumption that the G165/G166 deletion-C165 insertion is located in the 5' untranslated region of *PCLN-1* mRNA. Further support for this theory arises from sequence alignments of human paracellin-1 with bovine paracellin-1, which was recently identified (29,30). Human and bovine paracellin-1 exhibit very little homology in their amino-terminal amino acid sequences but share a suitable methionine at human amino acid position 71/bovine amino acid position 20, which is followed by amino acid sequences of high homology (91% identity and 95% similarity) for the complete length of the proteins (Figure 5). This finding strongly indicates that human paracellin-1 is considerably shorter than previously reported and lacks a major part of the amino terminus, similar to other members of the claudin family. This finding supports the hypothesis that the second methionine is the original translational start site. Alternatively, two different isoforms might exist in the kidney, resulting from two different translational start sites. It might be speculated that the shorter protein is able to prevent renal disease in individuals who are affected by the G165/G166 deletion-C165 insertion. It is hoped that additional studies on the translational regulation of paracellin-1 will resolve this controversy.

In summary, although much has been learned with respect to FHHNC pathophysiologic processes and the underlying genetic defect, new questions regarding aspects of the gene and protein structures have arisen. Additional basic studies on tight junction assembly and the proteins involved might answer some of these questions. With respect to the rapid deterioration of renal function in a great number of affected children, our understanding of the development of renal insufficiency in FHHNC must be extended. Therapeutic strategies, especially those targeting the prevention of ESRD, will hopefully improve in the future.

Acknowledgments

We are indebted to the participating patients and their families for their cooperation. We thank Nora Alffen and Ulla Pechmann for excellent technical assistance. Drs. Konrad and Seyberth were sup-

ported by the Deutsche Forschungsgemeinschaft (Ko1480/3-2). Dr. Weber was supported by the Stiftung P. E. Kempkes (Kennziffer 30/99).

References

- Cole DE, Quamme GA: Inherited disorders of renal magnesium handling. *J Am Soc Nephrol* 11: 1937–1947, 2000
- Geven WB, Monnens LA, Willems HL, Buijs WC, ter Haar BG: Renal magnesium wasting in two families with autosomal dominant inheritance. *Kidney Int* 31: 1140–1144, 1987
- Gitelman HJ, Graham JB, Welt LG: A new familial disorder characterized by hypokalemia and hypomagnesemia. *Trans Assoc Am Physicians* 79: 221–235, 1966
- Michelis MF, Drash AL, Linarelli LG, De Rubertis FR, Davis BB: Decreased bicarbonate threshold and renal magnesium wasting in a sibship with distal renal tubular acidosis: Evaluation of the pathophysiological role of parathyroid hormone. *Metabolism* 21: 905–920, 1972
- Castrillo JM, Rapado A, Traba ML, Esbrit P, Hernando L: Nephrocalcinosis con Hipomagnesemia. *Nefrologia*, 3: 159–165, 1983
- Benigno V, Canonica CS, Bettinelli A, von Vigier RO, Truttmann AC, Bianchetti MG: Hypomagnesaemia-hypercalciuria-nephrocalcinosis: A report of nine cases and a review. *Nephrol Dial Transplant* 15: 605–610, 2000
- Simon DB, Lu Y, Choate KA, Velazquez H, Al-Sabban E, Praga M, Casari G, Bettinelli A, Colussi G, Rodriguez-Soriano J, McCredie D, Milford D, Sanjad S, Lifton RP: Paracellin-1, a renal tight junction protein required for paracellular Mg^{2+} reabsorption. *Science (Washington DC)* 285: 103–106, 1999
- Weber S, Hoffmann K, Jeck N, Saar K, Boeswald M, Kuwertz-Broeking E, Meij II, Knoers NV, Cochat P, Sulakova T, Bonzel KE, Soergel M, Manz F, Schaerer K, Seyberth HW, Reis A, Konrad M: Familial hypomagnesaemia with hypercalciuria and nephrocalcinosis maps to chromosome 3q27 and is associated with mutations in the *PCLN-1* gene. *Eur J Hum Genet* 8: 414–422, 2000
- Gregoric A, Bracic K, Novljan G, Marcun-Varda N: Pseudotumor cerebri in a child with familial hypomagnesemia-hypercalciuria. *Pediatr Nephrol* 14: 269–270, 2000
- Manz F, Scharer K, Janka P, Lombeck J: Renal magnesium wasting, incomplete tubular acidosis, hypercalciuria and nephrocalcinosis in siblings. *Eur J Pediatr* 128: 67–79, 1978
- Rodriguez-Soriano J, Vallo A: Pathophysiology of the renal acidification defect present in the syndrome of familial hypomagnesaemia-hypercalciuria. *Pediatr Nephrol* 8: 431–435, 1994
- Praga M, Vara J, Gonzalez-Parra E, Andres A, Alamo C, Araque A, Ortiz A, Rodicio JL: Familial hypomagnesemia with hypercalciuria and nephrocalcinosis. *Kidney Int* 47: 1419–1425, 1995
- Ulmann A, Hadj S, Lacour B, Bourdeau A, Bader C: Renal magnesium and phosphate wastage in a patient with hypercalciuria and nephrocalcinosis: Effect of oral phosphorus and magnesium supplements. *Nephron* 40: 83–87, 1985
- Rodriguez-Soriano J, Vallo A, Garcia-Fuentes M: Hypomagnesaemia of hereditary renal origin. *Pediatr Nephrol* 1: 465–472, 1987
- Quamme GA: Renal magnesium handling: New insights in understanding old problems. *Kidney Int* 52: 1180–1195, 1997
- Morita K, Furuse M, Fujimoto K, Tsukita S: Claudin multigene family encoding four-transmembrane domain protein components of tight junction strands. *Proc Natl Acad Sci USA* 96: 511–516, 1999
- Geven WB, Monnens LA, Willems JL: Magnesium metabolism in childhood. *Miner Electrolyte Metab* 19: 308–313, 1993
- Moxey-Mims MM, Stapleton FB: Hypercalciuria and nephrocalcinosis in children. *Curr Opin Pediatr* 5: 186–190, 1993
- Matos V, van Melle G, Boulat O, Markert M, Bachmann C, Guignard JP: Urinary phosphate/creatinine, calcium/creatinine, and magnesium/creatinine ratios in a healthy pediatric population. *J Pediatr* 131: 252–257, 1997
- Schwartz GJ, Brion LP, Spitzer A: The use of plasma creatinine concentration for estimating glomerular filtration rate in infants, children, and adolescents. *Pediatr Clin North Am* 34: 571–590, 1987
- Orita M, Suzuki Y, Sekiya T, Hayashi K: Rapid and sensitive detection of point mutations and DNA polymorphisms using the polymerase chain reaction. *Genomics* 5: 874–879, 1989
- Dib C, Faure S, Fizames C, Samson D, Drouot N, Vignal A, Millasseau P, Marc S, Hazan J, Seboun E, Lathrop M, Gyapay G, Morissette J, Weissenbach J: A comprehensive genetic map of the human genome based on 5,264 microsatellites. *Nature (Lond)* 380: 152–154, 1996
- Wrong O: Nephrocalcinosis. In: *Oxford Textbook of Clinical Nephrology*, 2nd Ed., edited by Davison AM, Cameron JS, Grünfeld J-P, Kerr DNS, Ritz E, Winearls CG, Oxford, UK, Oxford University Press, 1998, pp 1376–1396
- Köckerling A, Reinalter SC, Seyberth HW: Impaired response to furosemide in hyperprostaglandin E syndrome: Evidence for a tubular defect in the loop of Henle. *J Pediatr* 129: 519–528, 1996
- Monnens L, Starremans P, Bindels R: Great strides in the understanding of renal magnesium and calcium reabsorption. *Nephrol Dial Transplant* 15: 568–571, 2000
- Furuse M, Fujita K, Hiiragi T, Fujimoto K, Tsukita S: Claudin-1 and -2: Novel integral membrane proteins localizing at tight junctions with no sequence similarity to occludin. *J Cell Biol* 141: 1539–1550, 1998
- Lemmink HH, Knoers NV, Karolyi L, van Dijk H, Niaudet P, Antignac C, Guay-Woodford LM, Goodyer PR, Carel JC, Hermes A, Seyberth HW, Monnens LA, van den Heuvel LP: Novel mutations in the thiazide-sensitive NaCl cotransporter gene in patients with Gitelman syndrome with predominant localization to the C-terminal domain. *Kidney Int* 54: 720–730, 1998
- Kozak M: Interpreting cDNA sequences: Some insights from studies on translation. *Mamm Genome* 7: 563–574, 1996
- Hirano T, Kobayashi N, Itoh T, Takasuga A, Nakamaru T, Hirotsune S, Sugimoto Y: Null mutation of *PCLN-1/claudin-16* results in bovine chronic interstitial nephritis. *Genome Res* 10: 659–663, 2000
- Ohba Y, Kitagawa H, Kitoh K, Sasaki Y, Takami M, Shinkai Y, Kunieda T: A deletion of the paracellin-1 gene is responsible for renal tubular dysplasia in cattle. *Genomics* 68: 229–236, 2000